Gate crashing arbuscular mycorrhizas:in vivoimaging shows the extensive colonization of both symbionts byTrichoderma atroviride

Gate crashing arbuscular mycorrhizas: *in vivo* imaging shows the extensive colonization of both symbionts by *Trichoderma atroviride*

Beatrice Lace[1], Andrea Genre[1], Sheridan Woo[2], A. Faccio[3], Matteo Lorito[2] & Paola Bonfante[1]

[1]Department of Life Science and Systems Biology, Università degli Studi di Torino, Viale Mattioli 25-10125 Torino, Italy;

[2]Department of Agriculture, Università degli Studi di Napoli Federico II

[3] Institute of Sustainable Plant Protection, CNR, Torino

Corresponding author: Paola Bonfante; Telephone: +00390116502927; Fax: +00390116705962; E-mail: paola.bonfante@unito.it

SUMMARY

Plant growth promoting fungi include strains of *Trichoderma* species that are used in biocontrol, and arbuscular mycorrhizal (AM) fungi, that enhance plant nutrition and stress resistance. The concurrent interaction of plants with these two groups of fungi affects crop performance, but has only been occasionally studied so far. Using *in vivo* imaging of GFP-tagged lines, we investigated the cellular interactions occurring between *Trichoderma atroviride* PKI1, *Medicago truncatula* and two *Gigaspora* species under *in vitro* culture conditions. *T. atroviride* did not activate symbiotic-like responses in the plant cells, such as nuclear calcium spiking or cytoplasmic aggregations at hyphal contact sites. Furthermore, *T. atroviride* parasitized *G. gigantea and G. margarita* hyphae through localized wall breaking and degradation - although this was not associated with significant chitin lysis nor the upregulation of two major chitinase genes. *T. atroviride* colonized broad areas of the root epidermis, in association with localized cell death. The infection of both symbionts was

This article has been accepted for publication and undergone full peer review but has not been through the copyediting, typesetting, pagination and proofreading process, which may lead to differences between this version and the Version of Record. Please cite this article as doi: 10.1111/1758-2229.12221

also observed when *T. atroviride* was applied to a pre-established AM symbiosis. We conclude that – although this triple interaction is known to improve plant growth in agricultural environments – in vitro culture brings to light a strong mycoparasitic potential for a biocontrol strain of *Trichoderma.*

INTRODUCTION

The release of plant root exudates in the rhizosphere attracts a multitude of microbes that thrive in this nutrient-rich niche. In addition to obligate biotrophs, like arbuscular mycorrhizal (AM) fungi belonging to Glomeromycota, the rhizosphere also hosts many facultative saprotrophic fungi. *Trichoderma/Hypocrea* spp. are present in soil, litter, dead wood, and are commonly isolated from the rhizosphere at all soil depths (Harman *et al.*, 2004). These fungi successfully exploit a multitude of substrates, supported by their large arsenal of poly- and oligo-saccharide hydrolytic enzymes (Druzhinina *et al.*, 2012). In particular, chitinases and glucanases allow *Trichoderma* species to act as mycotrophs that antagonize, parasitize and kill other fungi. This feature has made the genus *Trichoderma* a first-choice in biocontrol against fungal pathogens (Harman *et al*., 2004), with the most common biocontrol strains belonging to *T. harzianum, T. asperellum/asperelloides, T. hamatum, T. viride* and *T. atroviride* (Druzhinina *et al*., 2012). In addition, the direct interaction with root cells can trigger plant induced systemic resistance, another mechanism of disease control, (Harman *et al*., 2004). Evidence indicates that the association of *Trichoderma* species with plant roots can range from symbiosis (Lorito and Woo, 2014) to endophytism and facultative pathogenicity (Druzhinina *et al.*, 2012), and involves the exploitation of plant derived carbohydrates by the fungus (Vargas *et al.*, 2009). Altogether, *Trichoderma* strains are more and more used as biofertilizers for their ability to stimulate plant growth (Harman, 2011) and defenses (Palmieri *et al.,* 2012). Recently, several molecular determinants for such capabilities have been identified following the genomic and transcriptomic analyses of *T. reesei* (Martinez *et al.*, 2008), *T. virens* and *T. atroviride* (Kubicek *et al.*, 2011; Atanasova *et al.,* 2013).

When growing in the rhizosphere or on root surface, *Trichoderma* is expected to have frequent interactions with plant mutualistic symbionts such as AM fungi (Bonfante and Genre, 2010). Indeed, such interactions have been investigated in the past, but - depending on the experimental setup - the inoculation with both fungi either resulted in positive synergistic effects on plant health or the inhibition of plant growth (Chandanie *et al.*, 2009; Rousseau *et al*., 1996). Furthermore, *T. harzianum* has displayed mycoparasitic activity on *Rhizophagus* sp. inside alginate beads (De Jeager *et al*., 2011). In order to fine tune effective biological control strategies that exploit these beneficial rhizospheric fungi, a more thorough understanding of their complex interaction and relationship with the plants is required.

In this work, an *in vitro* method already established to monitor the early phases of the interaction between *Medicago truncatula* and *Gigaspora gigantea* (Genre *et al*., 2005; 2008; 2009) was extended to a triple system by adding a GFP-tagged strain of *Trichoderma atroviride* biocontrol isolate PKI1. We investigated the dual interaction between the two fungi and observed a mycoparasitic activity of the biocontrol agent, noticing that *T. atroviride* equally colonizes live and UV-killed AM hyphae; our results also indicate that mycoparasitism is not associated with extensive chitin lysis and two major *T. atroviride* chitinase genes (ECH42 and NAG1) are not significantly upregulated. Analyzing the dual interaction between *T. atroviride* and *M. truncatula*, we observed extensive hyphal colonization of root cells, associated with localized cell death; furthermore, *T. atroviride* PKI1 did not trigger plant symbiotic responses such as the activation of nuclear calcium spiking (Singh and Parniske, 2012) or prepenetration-associated cytoplasmic aggregations at hyphal contact sites (Genre *et al*., 2005; 2007). Lastly, by studying the triple interaction between *T. atroviride*, *G. gigantea* and *M. truncatula*, we concluded that the symbiotic condition does not protect the plant nor the glomeromycete from *T. atroviride* infection.

RESULTS

Trichoderma atroviride PKI1 parasitizes *Gigaspora gigantea*

When grown in dual interaction (see Materials and methods in Supplemental File 7 for a full description of the experimental setup) *T. atroviride* PKI1 and *G. gigantea* hyphae were clearly visualized and distinguishable in both stereo- and confocal microscopy, thanks to the constitutive green fluorescence of the GFP-tagged *T. atroviride* PKI1 mycelium and the strong autofluorescence of *G. gigantea* (Figure 1). Hyphae of *T. atroviride* were 4-5 µm in diameter, septate, in contrast to the larger (around 10 µm), aseptate hyphae of *G. gigantea*. Occasional septa could be spotted delimiting terminal hyphal section devoid of cytoplasm, as often observed in Glomeromycota hyphae arising from spore germination in the absence of a host plant. The first contacts between *G. gigantea and T. atroviride* hyphae (growing without apparent tropism) were observed 24 hours post-inoculation (hpi) as presented in Figure 1A. None of the specialized hyphal structures typically developed by *Trichoderma* during mycoparasitic and non-mycoparasitic interactions, such as coiling filaments or appressoria (Lu *et al.,* 2004), were observed at this time.

Transmission electron microscopy visualized the wall ultrastructure of both fungi at sites of hyphal contact. The wall was more electron-transparent in *T. atroviride* than *G. gigantea*, which displayed two distinct electron-dense layers and localized amorphous extrusions (Figures 2A and 2B).

At 48 hpi, *Trichoderma* deployed a widespread, highly branched mycelium, intermingling and overlapping the sparser *G. gigantea* hyphae. At this time, *T. atroviride* had penetrated and grown inside several hyphae of the glomeromycete (Figures 1B and 1C). Outbursts of the parasitized hypha cytoplasm were clearly visible around the perforation points (Figure 1B). Remarkably, *T. atroviride* hyphae formed clusters of short branches inside the extruded cytoplasm, protruding towards the damaged AM mycelium. Intra-hyphal growth of *T. atroviride* proceeded rapidly, possibly facilitated by the absence of septa (Figure 1C). Seventy-two hpi, *T. atroviride* had extensively colonized the inside of several *G. gigantea* hyphae, and wrapped around the glomeromycete auxiliary cells with short, convoluted hyphae (Figures 1D and 1E).

Transmission electron microscopy revealed that hyphal penetration sites were associated with a structural damage of the *G. gigantea* wall (Figure 2C): breaking points were observed in areas

where the inner electron-dense layer was reduced to a loose fibrillar network, although the outer amorphous extrusions showed no evident sign of degradation (Figure 2D). Importantly, the glomeromycete cytoplasm was reduced to a degenerated clump with no recognizable inner structure. Comparable senescence events in the AM fungus were never observed in control plates of the same age (Supplemental Figures 1A and 1B). By contrast, the mycoparasite hyphae displayed an active cytoplasm, very rich in organelles (Figure 2C).

Beside timing the phases of the *T. atroviride / G. gigantea* interaction, our combined confocal and electron microscopy observations demonstrate that *T. atroviride* can effectively mycoparasitize an AM fungus when grown in axenic dual cultures, with a major degradation of the glomeromycete cytoplasm and intense, local dismantling of the wall texture in the parasitized hyphae.

T. atroviride mycoparasitism is not associated with major chitinolytic activity

In order to assess whether local wall degradation was associated with chitin lysis by *T. atroviride* chitinases, we performed a cytochemical detection of chitin by applying gold-labelled wheat germ-agglutinin, a lectin that specifically binds chitin (Bonfante *et al*., 1990) on electron microscopy samples. As expected, both *Trichoderma atroviride* and *Gigaspora gigantea* cell walls resulted to be homogeneously labelled (Supplemental Figure 2). However, quantitative image analysis did not reveal any statistical difference in the gold granule amount between uncolonized and parasitized AM hyphae (Supplemental Figure 2D). This suggests that the observed wall dismantling does not significantly impact the chitin component.

This finding was further confirmed by experiments with two strains of *T. atroviride* espressing a cytoplasmic GFP under either the 42-kDa endochitinase promoter *(ech42::gfp)* or the β-N-acetylglucosaminidase promoter *(nag1::gfp)*. Both promoters are known to be activated when *Trichoderma* is grown in the presence of chitin as its major carbon source (Carsolio *et al.*, 1999; Brunner *et al*., 2003). When the two strains were grown in the presence of *G. gigantea,* the timing

and pattern of their infection process was the same as for PKI1. Fluorescence quantification showed no relevant change in the expression of *ech42* (endochitinase) during the whole time-course of the experiment, compared to the control; *nag1* (exochitinase) expression level was only weakly enhanced 24 hours post *T. atroviride* inoculation (earlier than the first hyphal contacts) and decreased to values lower than the control at 96 hpi, when contacts and mycoparasitic colonization were observed (see Supplemental Figures 3A and 3B).

The observation that two major chitinases of *T. atroviride* (an endo- and an exochitinase) were not significantly upregulated during the parasitic phase indirectly supports the results of wall chitin labelling experiments, suggesting that chitin lysis in the parasitized hyphal wall has not a major role in the mycoparasitic event.

Trichoderma atroviride mycoparasitism does not require viable host hyphae

To better understand whether the observed extensive hyphal colonization involves any active response by the AM fungus, the glomeromycete hyphae (*G. margarita*), was exposed to 90 min UV irradiation prior to inoculation of *T. atroviride*. The effective loss of viabiliy in the AM hyphae was assessed by confocal microscopy observations, which revealed the stop of all cytoplasmic streams (see Supplemental Movies 4 and 5). Importantly, no outbreak of cytoplasm was observed, indicating that *G. margarita* cell walls were intact. As in the previous experiments, the two fungi were clearly recognizable due to their distinct fluorescence wavelenghts (Figure 3). The time-course of the interaction was exactly the same as in the presence of the viable AM fungus. *Trichoderma* could be spotted inside *Gigaspora* hyphae starting from 48 hpi (Figures 3A and 3B); massive colonization sites were marked by multiple coiled hyphae completely filling the AM hyphal lumen (Figure 3A).

Interestingly, observations at 72 hpi showed *Trichoderma* preferentially growing in *Gigaspora* cytoplasm-filled hyphae, while avoiding empty hyphal branches (Figure 3C). A time-lapse sequence is shown in Figures 3D-3I (and Supplemental Movie 6), showing a *Trichoderma* hypha

proceeding all along a *Gigaspora* hypha and branching in correspondence of the parasitized hyphal branches. Subsequent profuse branching led to the occupation of most of the hyphal lumen (Figure 3H). The swelling of *Trichoderma* hyphal tip was evident as it reached the apex of the *Gigaspora* hypha (Figure 3H). Eventually, *T. atroviride* exited the *G. margarita* apex by perforating its terminal wall (Figure 3I).

These observations showed that *T. atroviride* is able to colonize both viable and non-viable AM hyphae, pointing out that no active response or signaling from *Gigaspora* is required to elicit the mycoparasitic process. In spite of its wide array of chitinolitic enzymes, *T. atroviride* preferentially grew in cytoplasm-filled hyphae. This suggests that *G. margarita* cytoplasm represents a more convenient substrate compared to the chitinous cell wall.

M. truncatula root colonization by _T. atroviride_ in dual cultures is associated with localized cell death

We used *M. truncatula* root organ cultures expressing the GFP-HDEL marker for the endoplasmic reticulum (ER) to assess plant cell viability and cytoplasm reorganization (Genre *et al*., 2009) during the dual interaction with *T. atroviride*. Twenty-four hours post inoculation, the fungus had grown diffusely, forming highly branched hyphae that extended radially from the inoculum plug (data not shown). At 48 hpi, isolated hyphae approached *M. truncatula* roots, but no direct contact was observed yet (Figure 4A). At this stage, root epidermal and cortical cells displayed a regular lace-like network of GFP-labelled ER cisternae, not different from control roots, indicating that hyphal vicinity did not affect cell viability (Figure 4B and Supplemental Figure 1D). At 72 hpi, the mycelium had almost entirely covered the Petri dish. Confocal microscopy revealed that the mycelium had extensively contacted the root epidermis (Figure 4C), but appressorium-like structures or root penetration events were never observed. Nevertheless, a partial disruption of the ER tubular structure was evident in epidermal and cortical cells, as GFP fluorescence was reduced to separate puncta and patches (Figure 4D). Cytoplasmic aggregations, typically observed in the

same experimental system upon contact with glomeromycetes or biotrophic pathogenic fungi (Genre *et al*., 2009), were never detected in the presence of *T. atroviride*. 144 hours post *T. atroviride* inoculation (6 days), the GFP-HDEL fluorescence had disappeared from all epidermal cells, indicating a significant loss of viability. As shown in Figure 4E and 4F, the cell borders were only marked by the reddish wall autofluorescence that in lively roots is covered by the bright GFP signal. The appearance of diffuse GFP fluorescence in the lumen of a few cells (Figure 4E and 4F) was likely due to more severe disruption of endocellular membranes. At this stage, single optical sections acquired from root inner focal planes revealed the presence of *T. atroviride* within the root tissues, growing inside the lumen of dead cells (Figure 4F). Control *M. truncatula* root cultures of the same age displayed a healthy ER with no cell death or other evident sign of senescence (see Supplemental Figures 1C and 1D).

These observations indicate that in our experimental conditions *T. atroviride* PKI1 acts as an endophytic root colonizer, causing localized cell death. Importantly, fungal contacts with the root epidermis do not trigger any of the pre-penetration cell responses typically observed during symbiotic or biotrophic pathogenic interactions: the formation of ER patches inside cytoplasmic aggregations at contact sites (Genre *et al.*, 2009) was in fact never observed.

T. atroviride **culture filtrates do not induce nuclear calcium signals in** ***M. truncatula***

We therefore decided to further investigate whether *T. atroviride* could activate early symbiotic responses in *M. truncatula*, A central element in the legume perception of both glomeromycetes and rhizobia is the so-called common symbiotic signaling pathway, or CSSP (Singh and Parniske, 2012). Its activation triggers persistent nuclear calcium oscillations known as calcium spiking (Sieberer *et al*., 2009; Chabaud *et al*., 2011). *T. atroviride* culture filtrates have previously been shown to activate defense-related responses (characteristic calcium signals and programmed cell death) in cells of soybean (Navazio *et al.,* 2007). On this basis, we applied an analogous *T. atroviride* culture filtrate to *M. truncatula* roots expressing the calcium-sensitive NUP-YC2.1

probe. Filtrates were obtained from *T. atroviride* cultures grown on either liquid M medium or sterile water: none of them triggered any variation in the nuclear calcium level of epidermal cells. As a positive control we used culture filtrates from *Gigaspora margarita*, which elicited intense nuclear calcium spiking, as expected (Chabaud *et al.*, 2011). Representative calcium plots are shown in Figure 5.

We conclude that *T. atroviride* exudates do not activate the CSSP in *M. truncatula* ROCs, suggesting that the plant is not perceiving *Trichoderma* diffusible signals through this conserved symbiotic pathway.

Root and hyphal colonization by *T. atroviride* is not influenced by the AM symbiotic status

In order to investigate the effect of *T. atroviride* on the symbiotic interaction *M. truncatula* / *G. gigantea*, mycorrhizal co-cultures were allowed to develop for 15 days before the inoculation with *T. atroviride*. AM establishment was monitored daily under a stereomicroscope and eventually confirmed by confocal microscopy. Root epidermal cells contacted by *G. gigantea* hyphae and hyphopodia displayed a healthy ER network, fully comparable to uninoculated control roots (Figure 6A). Similarly, intracellular hyphae were observed in healthy epidermal and cortical cells (Figure 6B). Lastly, several inner cortical cells contained fully developed arbuscules, confirming the active status of the symbiosis (as displayed in Figure 6C). *T. atroviride* developed profusely as early as 24 hpi, similarly to what was observed in the dual interaction experiments described above. Fourty-eight hours post *T. atroviride* inoculation, no direct contact was occurring and both *M. truncatula* epidermal cells and *G. gigantea* hyphae displayed a healthy aspect, fully comparable to controls (Figures 7A and 7B). *T. atroviride* hyphae spread over the root surface at 72 hpi and proliferated with particular intensity in the vicinity of *G. gigantea* (Figure 7C): branches and coils were observed at this stage around *G. gigantea* auxiliary cells (Figure 7D). Following contact with *T. atroviride*, several root cells had lost their GFP-HDEL fluorescence (Figure 7D). After 144 hours (6 days) the mycelium of *T. atroviride* had entirely covered the medium surface. Dense hyphal coils

had developed inside some of the auxiliary cells of *G. gigantea,* entirely filling their lumen (Figure 7F) and causing the loss of cytoplasmic autofluorescence (and, on that account, viability). Areas of epidermal cell death could be observed throughout the root system, which were almost completely void of GFP-HDEL fluorescence (Figure 7E). In accordance with our observations of dual interaction, penetration and coiling of *T. atroviride* hyphae inside the cortical cells of *M. truncatula* root was also detected (Figures 7G and 7H). Synchronous observation of control plates lacking *T. atroviride* inoculation showed that the active status of the AM mycorrhization persisted throughout the experimental period. In this case, the lace-like structure of the ER in *M. truncatula* epidermal cells, as well as the *G. gigantea* autofluorescence, were fully maintained (Supplemental Figures 1E and 1F), indicating no loss of viability for either symbiont.

Altogether, the development of *T. atroviride* infection, at least in terms of microscopic morphology, was not affected by the symbiotic status of the *M. truncatula* / *G. gigantea* interaction. The mycoparasite colonized *M. truncatula* roots, leading to localized cell death, and penetrated *G. gigantea* hyphae and auxiliary cells, thus affecting the viability of the AM fungus. In conclusion, the development of *T. atroviride* was fully comparable in the mycorrhizal (triple) and non-mycorrhizal (dual) interactions.

DISCUSSION

T. atroviride dismantles glomeromycetes wall and feeds on their cytoplasm

In our experimental conditions, *T. atroviride* PKI1 penetrated *G. gigantea* and *G. margarita* hyphae with localized cell wall dismantling, in analogy to the process described for other species of *Trichoderma* parasitizing the AM fungus *Rhizophagus irregularis* or several phytopathogens (Benhamou and Chet, 1997; Rousseau *et al*., 1996). Such processes have long been ascribed to the action of cell wall degrading enzymes - chitinases, glucanases and proteases - and secondary metabolites (Di Pietro *et al*., 1993; Lorito *et al*., 1993a; 1993b; 1994; 1996; Schirmböck *et al*., 1994; Zeilinger *et al*., 1999). This was supported by targeted gene knock-out or overexpression

256 experiments (Woo *et al*., 1999; Djonović *et al*., 2006; Djonović *et al*., 2007) and genome
257 sequencing of a few *Trichoderma* species (Martinez *et al.*, 2008; Kubicek *et al.*, 2011), where a
258 huge inventory of genes encoding poly- and oligosaccharide hydrolytic enzymes has been found
259 (Druzhinina *et al.*, 2012). Nevertheless, a genome-wide expression study has indicated that *T.*
260 *atroviride* mostly expresses glucanases belonging to the GH16 family and proteases during
261 *Rhizoctonia solani* colonization (Atanasova *et al*., 2013), suggesting that chitinases are not major
262 determinants of mycoparasitism in this species. Our results are in line with this view and show that
263 *T. atroviride* can enter the complex multilayered wall of a Gigasporacean AM fungus – reportedly
264 composed of chitin, beta 1-4 glucans, mannans and proteins (Bonfante, 2001; Tisserant *et al.*,
265 2013). Nevertheless, the dismantling of the glomeromycete cell wall was only evident at penetration
266 sites, in the immediate vicinity of intra-hyphal hyphae. Wall degradation mainly involved the
267 electron dense components of the wall, exposing a loose fibrillar network, probably representing the
268 untouched chitin skeleton. This appears to be sufficient to grant wall loosening and access of the
269 mycoparasite to the coenocytic hyphal lumen. The fact that both major chitinases of *T. atroviride*
270 were not upregulated during its interaction with the AM fungus - as highlighted by our experiments
271 with *ech42::gfp* and *nag1::gfp* strains - indirectly supports this hypothesis.
272 Furthermore, our experiments with UV-killed *Gigaspora margarita* show that *T. atroviride* does
273 not require any active response by the glomeromycete to start its colonization. Moreover, the
274 colonization of living AM fungal hyphae followed exactly the same timing and pattern, suggesting
275 that AM hyphae are prone to *T. atroviride* mycoparasitism.
276
277 **_T. atroviride_ causes root cell death**
278 *Trichoderma spp.* are free-living fungi, widespread in soil and root ecosystems, but selected strains
279 are widely used in agriculture because of their beneficial effect on plant stress response and yield.
280 This led to the description of *Trichoderma* species as beneficial - or even symbiotic - plant growth

promoters (Harman, 2000; 2011; Harman *et al.*, 2004; Chacon *et al.*, 2007). However local cellular and molecular responses to *Trichoderma* colonization are not fully understood or, in the case of *T. atroviride,* completely unknown.

Our live observation of *T. atroviride* / *M. truncatula* interaction shows that *T. atroviride* exudates do not trigger typical symbiotic responses such as the activation of the CSSP pathway or the assembly of cytoplasmic aggregations at hyphal contact sites (Genre *et al*., 2005; 2009). In contrast with this early stealth approach, *T. atroviride* causes localized plant cell death within six days post inoculation - similarly to what has been described upon the attack by the necrotrophic fungus *Phoma medicaginis* (Genre *et al*., 2009). Such cell death responses, including programmed cell death and leading to the formation of necrotic areas, have sometimes been observed, although not fully characterized, in several *Trichoderma*-treated plants at root and seed surface (Howell, 2006 and Howell C. personal communication). Significantly, such responses are more evident when the interaction is established *in vitro*, on sugar-rich substrates, or when the secreted metabolites are used instead of the living fungus (Navazio *et al*., 2007). It is a common understanding that, under natural conditions, local root lesions caused by these beneficial microbes are indeed tolerated by the plant. Necrotic lesions have been proposed to be necessary for achieving the "priming" effect, by which several *Trichoderma* strains activate plant defense responses to 'true' pathogens (Brotman *et al*., 2012; 2013; Tucci *et al*., 2011; Palmieri *et al*., 2012). Similarly, Deshmukh *et al.* (2006) demonstrated that the endophyte *Piriformospora indica,* known to promote growth on a broad spectrum of host plants (Schäfer *et al.*, 2007), also requires cells death for its successful proliferation in differentiated barley roots.

Recent studies have demonstrated the extensive "reprogramming" of host plant physiology following the establishment of a successful root colonization by effective *Trichoderma* strains, as noted on both the expressome and the proteome (Harman, 2011; Lorito *et al*., 2010; Morán-Diez *et*

al., 2012; Shoresh *et al*., 2010; Perazzoli *et al*., 2012). A targeted gene expression study on plant cell death markers should finally demonstrate if (programmed) cell death is a necessary step at least in some plant-*Trichoderma* interactions to activate systemic resistance or growth promotion responses. For sure, the contrast is striking with the root colonization mechanism in AM, where the preservation of plant cell integrity is required for fungal penetration and symbiosis establishment (Bonfante and Genre, 2010).

Arbuscular mycorrhiza does not alleviate *T. atroviride*-induced damage on either *M. truncatula* or *G. gigantea*

DeJaeger *et al*. (2010) studied the mycoparasitic interaction between *T. harzianum* and *G. intraradices,* and reported that intraradical AM mycelium colonizing potato roots was susceptible to *T. harzianum* invasion. In their experimental conditions, the presence of the AM fungus seems to be required for root penetration by *T. harzianum*, with no apparent detrimental effects on either the plant or the AM fungus. By contrast, our results show that *T. atroviride* can directly colonize root tissues - regardless of the presence of an AM fungus - and affect the viability of both *G. gigantea* hyphae and *M. truncatula* root cells. Furthermore, confocal microscopy never showed the presence of *T. atroviride* inside the intraradical mycelium of *G. gigantea,* in apparent contradiction with the hypothesis that *Trichoderma* spp. exploit the glomeromycete mycelium as an access route to inner root tissues. This contrasting evidence could be due to the different fungal and plant species, as well as to the high level of adaptability of these ecologically successful root-associated microbes. In fact, DeJaeger and colleagues (2010) had purposely chosen a strain of *T. harzianum* known for its inability to penetrate the roots of *S. tuberosum*, in order to highlight the intraradical AM mycelium-mediated colonization mechanism. It should also be noted that our experimental setup imposes the use of root organ cultures lacking the aerial part of the plant. As a consequence, systemic and physiological responses due to the combined action of the two fungi (Martínez-Medina *et al*., 2011)

could not be taken into account. We cannot exclude that *in vitro* conditions gave *Trichoderma* a particularly favourable environment to deploy its mycoparasitic and plant necrotrophic strategies. Further studies can now be envisaged to assess the importance of these phenomena in natural conditions, where the complexity and competitiveness of the rhizosperic environment may mitigate the aggressiveness that *Trichoderma* displayed in our *in vitro* conditions.

In conclusion, a combination of detailed live imaging, electron microscopy studies and live gene expression analyses of the interactions between a biocontrol strain of *Trichoderma* and plant/fungal AM partners, revealed several unexpected features, providing novel clues for the understanding of such complex interactions. In this line, our cell-biology based results nicely complement the recent transcriptomic data produced after *Trichoderma* genome sequencing.

Acknowledgments

The authors express their thank to Dr. R. W. Roberson, (SOLS, Arizona State University) for advices on electron microscopy fixation protocols and to Dr. M. Novero for her assistance with statistical analyses. Research was funded by MIUR-PRIN 2008 project to PB and ML.

BL performed all experiments, analyzed the data and contributed to the writing; AG performed confocal microscopy experiments, analyzed the data and contributed to the writing; AF performed the electron microscopy experiments; SW and ML analyzed the data and contributed to the writing; PB conceived the experimental design; analyzed the data and wrote the manuscript.

LITERATURE CITED

Atanasova L., Le Crom S., Gruber S., Coulpier F., Seidl-Seiboth V., Kubicek C. P. and Druzhinina I. P. 2013. Comparative transcriptomics reveals different strategies of *Trichoderma* mycoparasitism. BMC Genomics 14, 121.

Bécard, G. and Fortin, J.A. 1988. Early events of vesicular-arbuscular mycorrhiza formation on Ri T-DNA transformed roots. New Phytol. 108, 211–18.

Benhamou, N. and Chet, I. 1997. Cellular and molecular mechanisms involved in the interaction between *Trichoderma harzianum* and *Pythium ultimum*. Appl. Environ. Microbiol. 63, 2095–2099.

Boisson-Dernier, A., Chabaud, M., Garcia, F., Bécard, G., Rosenberg, C., Barker, DG. 2001. *Agrobacterium rhizogenes*-transformed roots of *Medicago truncatula* for the study of nitrogen-fixing and endomycorrhizal symbiotic associations. MPMI 14, 695–700.

Bonfante, P., Vian, B., Perotto, S., Faccio, A., Knox, J.P. 1990. Cellulose and pectin localization in roots of mycorrhizal *Allium porrum*: labelling continuity between host cell wall and interfacial material. Planta 180, 537–547.

Bonfante, P. 2001. At the interface between mycorrhizal fungi and plants: the structural organization of cell wall, plasma membrane and cytoskeleton. In: Hock B (ed) The Mycota IX. Fungal associations. Springer, Berlin, 45–91.

Bonfante, P. & Genre, A. 2010. Mechanisms underlying beneficial plant-fungus interactions in mycorrhizal symbiosis. Nat commun. 1, 48.

Brotman,Y., Lisec, J., Méret, M., Chet, I., Willmitzer, L., Viterbo, A. 2012. Transcript and metabolite analysis of the *Trichoderma*-induced systemic resistance response to *Pseudomonas syringae* in Arabidopsis thaliana. Microbiology 22, 139–146.

Brotman, Y., Landau, U., Cuadros-Inostroza, Á., Takayuki, T., Fernie, A.R., *et al*. 2013. *Trichoderma*-plant root colonization: escaping early plant defense responses and activation of the antioxidant machinery for saline stress tolerance. PLoS Pathog 9(3): e1003221.

Brunner, K., Peterbauer, C. K., Mach, R. L., Lorito, M., Zeilinger, S., Kubicek, C. P. 2003. The Nag1 *N*-acetylglucosaminidase of *Trichoderma atroviride* is essential for chitinase induction by chitin and of major relevance to biocontrol. Curr. Genet. 43, 289-295.

Carsolio, C., Benhamou, N., Haran, S., Cortés, C., Gutiérrez, A., Chet, I., Herrera-Estrella, A. 1999. Role of the *Trichoderma harzianum* endochitinase gene, *ech42*, in mycoparasitism. Appl. Environ. Microbiol. 65, 929-935.

Chabaud, M., Venard, C. & Barker, D. G. 2002. Targeted inoculation of *Medicago truncatula* in vitro root cultures reveals MtENOD11 expression during early stages of infection by arbuscular mycorrhizal fungi. New Phytol., 156, 265–273.

Chabaud, M., Genre, A., Sieberer, B. J., Faccio, A., Fournier, J., Novero, M., Barker, D.G., Bonfante, P. 2011. Arbuscular mycorrhizal hyphopodia and germinated spore exudates trigger Ca^{2+}

399 spiking in the legume and nonlegume root epidermis. New Phytol 189, 347-55.
400
401 Chacon, M.R., Rodríguez-Galán, O., Benítez, T., Sousa, S., Rey, M., Llobell, A., Delgado-Jarana,
402 J. 2007. Microscopic and transcriptome analyses of early colonization of tomato roots by
403 *Trichoderma harzianum*. Int. Microbiol 10,19–27.
404
405 Chandanie, W.A., Kubota, M., Hyakumachi, M. 2009. Interactions between the arbuscular
406 mycorrhizal fungus *Glomus mosseae* and plant growth-promoting fungi and their significance for
407 enhancing plant growth and suppressing damping-off of cucumber (*Cucumis sativus* L.). App Soil
408 Ecol 41, 336-341.
409
410 De Jaeger, N., Declerck, S., De la Providencia, I. E. 2010. Mycoparasitism of arbuscular
411 mycorrhizal fungi: a pathway for the entry of saprotrophic fungi into roots. FEMS microbiol ecolol
412 73, 312–22.
413
414 De Jaeger, N., de la Providencia, I. E., Rouhier, H., Declerck, S. 2011. Co-entrapment of
415 *Trichoderma harzianum* and *Glomus sp*. within alginate beads: impact on the arbuscular
416 mycorrhizal fungi life cycle. J Appl microbiol 111, 125–35.
417
418 Deshmukh, S., Hückelhoven, R., Schäfer, P., Imani, J., Sharma, M., Weiss, M., Waller, F., Kogel,
419 K.H. 2006. The root endophytic fungus *Piriformospora indica* requires host cell death for
420 proliferation during mutualistic symbiosis with barley. PNAS 103, 18450-7.
421

Di Pietro A., Lorito, M., Hayes, C.K., Broadway R.M. and Harman, G.E. 1993. Endochitinase from *Gliocladium virens*: isolation, characterization and synergistic antifungal activity in combination with gliotoxin. Phytopathology 83, 308-313.

Djonović, S., Pozo, M.J., Kenerley, C.M. 2006. Tvbgn3, a beta-1,6-glucanase from the biocontrol fungus *Trichoderma virens*, is involved in mycoparasitism and control of *Pythium ultimum*. Appl Environ Microbiol. 72, 7661-70.

Djonović, S., Vittone, G., Mendoza-Herrera, A., Kenerley, C.M. 2007. Enhanced biocontrol activity of *Trichoderma virens* transformants constitutively coexpressing beta-1,3- and beta-1,6-glucanase genes. Mol Plant Pathol. 8, 469-80.

Druzhinina, I. S., Shelest, E. & Kubicek, C. P. 2012. Novel traits of *Trichoderma* predicted through the analysis of its secretome. FEMS Microbiol Lett 337, 1-9.

Genre, A., Chabaud, M., Timmers, T., Bonfante, P. & Barker, D. G. 2005. Arbuscular mycorrhizal fungi elicit a novel intracellular apparatus in *Medicago truncatula* root epidermal cells before infection. Plant cell online 17, 3489.

Genre, A., Bonfante, P. 2007. Check-in procedures for plant cell entry by biotrophic microbes. MPMI 20, 1023-1030.

Genre, A., Chabaud, M., Faccio, A., Barker, D. G. & Bonfante, P. 2008. Prepenetration apparatus assembly precedes and predicts the colonization patterns of arbuscular mycorrhizal fungi within the

446 root cortex of both *Medicago truncatula* and *Daucus carota*. Plant cell 20, 1407–20.

447

448 Genre, A., Ortu, G., Bertoldo, C., Martino, E. & Bonfante, P. 2009. Biotic and abiotic stimulation
449 of root epidermal cells reveals common and specific responses to arbuscular mycorrhizal fungi.
450 Plant physiol. 149, 1424-34.

451

452 Harman, G.E. 2000. Myths and dogmas of biocontrol. Changes in perceptions derived from
453 research on *Trichoderma harzianum* T22. Plant disease 84, 377–393.

454

455 Harman, G.E., Howell, C.R., Viterbo, A., Chet, I. & Lorito, M. 2004. *Trichoderma* species-
456 opportunistic, avirulent plant symbionts. Nat Rev Microbiol 2, 43-56.

457

458 Harman, G.E. 2011. Multifunctional fungal plant symbionts: new tools to enhance plant growth and
459 productivity. New Phytol. 189, 647-9.

460

461 Hoch, H.C. 1986. Freeze-substitution of fungi. In: Aldrich HC, Todd WJ, eds. Ultrastructure
462 techniques of microorganisms. New York: Plenum Press, 183–211.

463

464 Howard, R.J., O'Donnell, K.L. 1987. Freeze substitution of fungi for cytological analysis. Exp
465 Mycol. 11, 250– 269.

466

467 Howell, C.R. 2006. Understanding the mechanisms employed by *Trichoderma virens* to effect
468 biological control of cotton diseases. Phytopathology 96, 178-80.

Kubicek, C. P. *et al*. 2011. Comparative genome sequence analysis underscores mycoparasitism as the ancestral life style of *Trichoderma.* Genome biol. 12, R40.

Lorito, M., Harman, G.E., Hayes, C.K., Broadway, R.M., Tronsmo, A., Woo, S.L. and Di Pietro, A. 1993a. Chitinolytic enzymes produced by *Trichoderma harzianum*: antifungal activity of purified endochitinase and chitobiosidase. Phytopathology 83, 302-307.

Lorito, M., Di Pietro, A., Hayes, C.K., Woo, S., Harman, G.E. 1993b. Antifungal, synergistic interaction between chitinolytic enzymes from *Trichoderma harzianum* and *Enterobacter cloacae*. Phytopatology 83, 721-728.

Lorito M., Hayes, C.K., Di Pietro, A., Woo, S.L. and Harman, G.E. 1994. Purification, characterization and synergistic activity of a glucan 1,3-ß-glucosidase and an N-acetyl-ß-glucosaminidase from *Trichoderma harzianum*. Phytopathology 84, 398-405.

Lorito, M., Farkas, V., Rebuffat, S., Bodo, B., Kubicek, C.P. 1996. Cell wall synthesis is a major target of mycoparasitic antagonism by *Trichoderma harzianum*. J Bacteriol. 178, 6382-5.

Lorito, M., Woo, S.L., Harman, G.E., Monte, E. 2010. Translational research on *Trichoderma*: from 'omics to the field. Annu Rev Phytopathol. 48, 395-417.

Lorito, M, and Woo, S.L. 2014. *Trichoderma*: a multi-purpose tool for IPM, in Principles of Plant-Microbe Interactions, Ed. B. Lugtenberg. Springer (in press).

494 Lu, Z., Tombolini, R., Woo, S., Lorito, M., Jansson, J.K., Zeilinger, S. 2004. In vivo study of
495 *Trichoderma*-pathogen-plant interactions using constitutive and inducible green fluorescent protein
496 reporter. Appl Environ Microbiol. 70, 3073.
497
498 Martinez, D. *et al*. 2008. Genome sequencing and analysis of the biomass-degrading fungus
499 *Trichoderma reesei* (syn. *Hypocrea jecorina*). Nat biotechnol. 26, 553-60.
500
501 Martínez-Medina, A., Roldán, A., Albacete, A. & Pascual, J. 2011. The interaction with arbuscular
502 mycorrhizal fungi or *Trichoderma harzianum* alters the shoot hormonal profile in melon plants.
503 Phytochemistry 72, 223–9.
504
505 Miyawaki, A., Llopis, J., Heim, R., Mccaffery, J.M., Adams, J.A., Ikurak, M., Tsien, R.Y. 1997.
506 Fluorescent indicators for Ca^{2+} based on green fluorescent proteins and calmodulin. Nature 388,
507 882-887.
508
509 Miyawaki, A., Griesbeck, O., Heim, R. & Tsien, R.Y. 1999. Dynamic and quantitative Ca^{2+}
510 measurements using improved cameleons. PNAS 96, 2135-40.
511
512 Morán-Diez, E., Rubio, B., Domínguez, S., Hermosa, R., Monte, E., Nicolás, C. 2012.
513 Transcriptomic response of *Arabidopsis thaliana* after 24 h incubation with the biocontrol fungus
514 *Trichoderma harzianum*. J Plant Physiol. 169, 614-20.
515
516 Navazio, L., Baldan, B., Moscatiello, R., Woo, S.L., Mariani, P., Lorito, M. 2007. Calcium-
517 mediated perception and defense responses activated in plant cells by metabolite mixtures secreted

by the biocontrol fungus *Trichoderma atroviride*. BMC Plant biol 7, 41.

Palmieri, M.C., Perazzolli, M., Matafora, V., Moretto, M., Bachi, A., Pertot, I. 2012. Proteomic analysis of grapevine resistance induced by *Trichoderma harzianum* T39 reveals specific defence pathways activated against downy mildew. J Exp Bot. 63, 6237-51.

Perazzolli, M., Moretto, M., Fontana, P., Ferrarini, A., Velasco, R., Moser, C., Delledonne, M. and Pertot, I. 2012. Downy mildew resistance induced by *Trichoderma harzianum* T39 in susceptible grapevines partially mimics transcriptional changes of resistant genotypes. BMC Genomics, 13: 660.

Reynolds, E.W. 1963. The use of lead citrate at high pH as an electron opaque stain in electron microscopy. J Cell Biol 17, 208-212.

Rousseau, A., Benhamou, N., Chet, I. & Piché Y. 1996. Mycoparasitism of the extramatrical phase of *Glomus intraradices* by *Trichoderma harzianum*. Phytopathology 86, 434–443.

Schäfer, P., Khatabi, B. & Kogel, K.H. 2007. Root cell death and systemic effects of *Piriformospora indica*: a study on mutualism. FEMS microbiol let. 275, 1–7.

Schirmböck , M., Lorito, M., Wang, Y.L., Hayes, C.K., Arisan-Atac, I., Scala, F., Harman, G.E., Kubicek, C.P. 1994. Parallel formation and synergism of hydrolytic enzymes and peptaibol

antibiotics, molecular mechanisms involved in the antagonistic action of *Trichoderma harzianum* against phytopathogenic fungi. Appl Environ Microbiol. 60, 4364-70.

Séjalon-Delmas, N., Magnier, A., Douds, D.D., Jr., and Bécard, G. 1998. Cytoplasmic autofluorescence of an arbuscular mycorrhizal fungus *Gigaspora gigantea* and nondestructive fungal observations in planta. Mycologia 90, 921–926.

Shoresh, M., Harman, G.E., Mastouri, F. 2010. Induced systemic resistance and plant responses to fungal biocontrol agents. Annu Rev Phytopathol. 48, 21-43.

Sieberer, B.J., Chabaud, M., Timmers, A.C., Monin, A., Fournier, J. and Barker, D.G. 2009. A nuclear-targeted cameleon demonstrates intranuclear Ca^{2+} spiking in *Medicago truncatula* root hairs in response to rhizobial nodulation factors. Plant physiol 151, 1197-206.

Singh, S. and Parniske, M. 2012. Activation of calcium- and calmodulin-dependent protein kinase (CCaMK), the central regulator of plant root endosymbiosis. Curr Opin Plant Biol. 15, 444–453.

Tisserant, E. *et al*. 2013. Genome of an arbuscular mycorrhizal fungus provides insight into the oldest plant symbiosis. Proc Natl Acad Sci 110, 20117-22.

Tucci, M., Ruocco, M., De Masi, L., De Palma, M., Lorito, M. 2011. The beneficial effect of *Trichoderma spp*. on tomato is modulated by the plant genotype. Mol Plant Pathol. 12, 341-54.

Vargas, W.A., Mandawe, J.C., Kenerley, C.M. 2009. Plant-derived sucrose is a key element in the

564 symbiotic association between *Trichoderma virens* and maize plants. Plant Physiol. 151, 792-808.

565

566 Woo, S.L., Donzelli, B., Scala, F., Mach, R., Harman, G.E., Kubicek , C.P., Del Sorbo, G. and
567 Lorito, M. 1999. Disruption of the *ech42* (endochitinase-encoding) gene affects biocontrol activity
568 in *Trichoderma harzianum* P1. MPMI 12, 419-429.

569

570 Zeilinger, S., Galhaup, C., Payer, K., Woo, S.L., Mach, R.L., Fekete, C., Lorito, M., and Kubicek,
571 C.P. 1999. Chitinase gene expression during mycoparasitic interaction of *Trichoderma harzianum*
572 with its host. Fungal Genet. Biol. 26, 131–140.

573

574 FIGURE CAPTIONS

575

576 **Figure 1.** Interaction of *Trichoderma atroviride* strain P1 expressing the GFP protein (mutant
577 PKI1) (green) with the autofluorescent AM fungus *Gigaspora gigantea* (red), observed in confocal
578 laser microscopy 24 (A), 48 (B and C) and 72 (D and E) hours post inoculation. A, Contact between
579 hyphae of *T. atroviride* (Ta), and *G. gigantea* (Gg). No specialized adhesion structures are
580 recognizable associated with hyphal contact. B, Images of *G. gigantea* cytoplasmic rupture
581 (asterisk) observed in fluorescence (top) and transmitted light (bottom) microscopy; presumably
582 due to perforation of the hyphal cell wall by *T. atroviride* hyphae. The hypha of PKI1 is visible
583 inside the AM fungal hypha (double arrowhead). Note the cluster of short branches (arrowheads) of
584 PKI1 hyphae developed towards *G. gigantea* cytoplasmic outburst. C, *T. atroviride* (double
585 arrowheads) growing inside a hypha of *G. gigantea* (dotted line), almost devoid of cytoplasm (as
586 indicated by its low fluorescence), observed under fluorescence (top) and transmitted light
587 (bottom). D, Extensive growth of *T. atroviride* mycelium around and inside *G. gigantea* hyphae and
588 auxilliary cells (ac). E, Higher magnification of the area outlined in D, showing *T. atroviride*

589 hyphae (arrowheads) growing inside the cytoplasm of *G. gigantea* hyphae (h) and auxiliary cells
590 (ac). Bars = 25μm

591

592 **Figure 2.** Transmission electron microscopy images of the dual interaction between *Trichoderma*
593 *atroviride* and *Gigaspora gigantea.* A, Direct contact between the two fungal walls (arrow and
594 boxed area). Both *T. atroviride* (Ta) and *G. gigantea* (Gg) hyphae have healthy cytoplasms with
595 easily recognizable organelles: intact nuclei (n), lipid globules (L) and electron dense granules
596 (arrowheads). B, Higher magnification of the area boxed in A, showing the contact between the
597 electron-transparent wall of *T. atroviride* (arrowhead) and the electron-dense wall of *G. gigantea*
598 (arrow) displaying two distinct dark layers. Amorphous masses (double arrowheads) emerge from
599 the outer layer of the AM fungus. C, *G. gigantea* hypha colonized by *T. atroviride*. The AM hyphal
600 wall is partially degraded (arrow and boxed area); cytoplasm is collapsed into a degenerated mass
601 (arrowhead), and the organelles are no longer distinguishable; by contrast, *T. atroviride* hyphae (Ta)
602 appear healthy and active, displaying nuclei (n) and lipid globules (L). D, Higher magnification of
603 the area boxed in C, showing a site of wall damage in *G. gigantea*: the inner electron-dense layer is
604 replaced by a loose fibrillar matrix (arrow). By contrast, the wall external layer and amorphous
605 masses (double arrowhead) are not degraded. Bars = 2 μm (A and C); 1 μm (B and D).

606

607 **Figure 3.** Interaction of *Trichoderma atroviride* PKI (green) with non-viable (UV-treated) hyphae
608 of *Gigaspora margarita* (red), observed in confocal microscopy after inoculation of *T. atroviride*.
609 A, B 48 hpi, *T. atroviride* (green) extensively colonized *G. margarita* (red) with intra-hyphal coils
610 (arrowhead). C Preferential growth of *T. atroviride* inside cytoplasm-filled hyphae of *G. margarita*
611 (arrowhead) observed in fluorescence (right) and transmitted light (left) 72 hpi: a hyphal branch
612 devoid of cytoplasm (asterisk), delimited by a septum (dotted line), is not colonized by *T.*
613 *atroviride.* D-I, Time-lapse series (total duration = 2h20') showing *T. atroviride* growing inside *G.*

margarita hyphae. D-F, Branching of *T.atroviride* within a *G. margarita* hyphal branch (arrows). H-I. Swelling and outbreak of *T.atroviride* hyphal tip at the apex of the *G. margarita* hypha (double arrowheads). Note the profuse branching of *T. atroviride* (H, arrowheads) inside the parasitized hyphae. Bars = 20μm

Figure 4. Dual interaction of *Trichoderma atroviride* PKI1 constitutively expressing cytoplasmic GFP (green) with root organ cultures of *Medicago truncatula* expressing GFP-HDEL as a marker of the endoplasmic reticulum. All images are obtained in confocal microscopy. A, B, 48 hpi of *T. atroviride,* a hypha (arrowhead) is approaching *M. truncatula* root. The intense fluorescence and integrity of the endoplasmic reticulum lace-like network (B) is a clear indicator of plant cell viability. C, D, 72 hpi, hyphae of the rapidly expanding *T. atroviride* mycelium overlap and coil around the root. Several contacts between hyphae and the root epidermis are visible (arrowheads) but no specialized adhesion structure is recognizable. The partial disorganization of the endoplasmic reticulum is evident in D, in the form of isolated patches and spots of GFP fluorescence. E, F, Six days after *T. atroviride* inoculum, most of the contacted epidermal cells are dead, as indicated by the partial to total disruption of the endoplasmic reticulum, and the disappearance or diffusion (arrow) of GFP fluorescence. Some of the hyphae are visible in F, coiling inside an epidermal cell (asterisk) and growing from cell to cell (double arrowhead). The weak red fluorescence of the plant cell walls becomes apparent in these images due to the absence of the bright GFP signal. Bars = 75 μm (A, C, E); 12μm (B, D, F).

Figure 5. Fluorescence resonance energy transfer (FRET) plots representing nuclear Ca^{2+} levels in epidermal cells of *Medicago truncatula* root organ cultures treated with culture filtrates of *Gigaspora margarita* (A), *Trichoderma atroviride* PKI1 (B), or sterile water as control (C). A, Treatment with 10 times concentrated exudate from germinated *Gigaspora margarita* spores elicits

intense spiking over the 40-min acquisition period. B, By contrast, no oscillation is visible in the plots from roots exposed to 10 times concentrated *T. atroviride* culture filtrates. C, No Ca^{2+} signals are elicited in control treatments with sterile water.

Figure 6. AM colonization of *Medicago truncatula* GFP-HDEL root organ cultures by *Gigaspora gigantea* before the inoculation of *Trichoderma atroviride* PKI1, observed in confocal microscopy. A, *Gigaspora gigantea* hyphopodium (double arrowhead) adhering to the root epidermis. Root cells display a healthy endoplasmic reticulum (note that GFP labelling extends to the nuclear envelope (n). B, Single optical section from the root cortical tissue. Cells colonized by *G. gigantea* hyphae (outlined by dotted lines) have an intact nucleus (n) and endoplasmic reticulum network (arrowhead). C, Optical section from an inner cortical cell hosting an arbuscule (ar), indicative of the active status of the symbiosis. The large nucleus (n) and arbuscule branches are surrounded by the intense GFP signal accumulated in the lumen of the nuclear envelope and ER respectively. Bars = 25µm.

Figure 7. Triple interaction between *Trichoderma atroviride* strain PKI1 and root organ cultures of *Medicago truncatula* previously colonized by *Gigaspora gigantea*. Fluorescent labeling and color coding are the same as in previous Figures. A, 48 hpi of *T. atroviride* (green), the first hyphae approach the root epidermis (arrowhead). Root epidermal cells and hyphae and auxilliary cells (ac) of *G. gigantea* are fully viable, as indicated by their respective green and red fluorescence. B, Detail of a few epidermal cells showing the integrity of their GFP-labelled endoplasmic reticulum. C, The diffuse branching of *T. atroviride* hyphae towards *G. gigantea* (arrowhead) is evident 72 hpi. D, A higher magnification shows *T. atroviride* hyphae coiling around an auxiliary cell of *G. gigantea* (arrow). In the same image, epidermal cells in the vicinity of *T. atroviride* hyphae display a diffuse fluorescence (asterisk) or complete loss of the GFP signal (arrowhead), indicative of endoplasmic

reticulum disruption and cell death. E, 144 hpi, the loss of epidermal cells viability is evident in the entire contact area, as indicated by the disappearance of GFP fluorescence. F, A higher magnification shows several hyphae of *T. atroviride* (arrows) growing inside the auxilliary cells of *G. gigantea*. G, An optical section from the root inner tissues at the same time interval shows that the endoplasmic reticulum structure is also lost in most cortical cells, including one that hosts *T.* atroviride hyphae (arrow). H, A higher magnification of the same spot shows the details of ER remnants in the form of small GFP-labelled puncta (arrowheads) spread in the cell lumen. *T. atroviride* coils inside the lumen of a dead cell (arrow). Bars = 75 μm (A, B, C, D); 25μm (G, H).

Suppl. Figure 1. Confocal microscopy images of *M. truncatula* GFP-HDEL and *G. gigantea* in the absence of *T. atroviride*. The pictures in A, C and E were recorded at the time of *T. atroviride* inoculation in the corresponding triple cultures (0 hpi), while the images shown in B, D and F correspond to the end point of the experiment (144 hpi). A, B, *Gigaspora gigantea* extraradical hyphae and auxiliary cells (ac) display a strong cytoplasmic fluorescence. C, D, *M. truncatula* root epidermal cells from an axenic culture display undamaged nuclei (arrowheads) and GFP-tagged endoplasmic reticulum, indicative of cell health. E, *G. gigantea* hyphopodium (arrow) adhesion to the root epidermis does not affect cell viability, as confirmed by endoplasmic reticulum integrity. F, Optical section from an inner cortical cell hosting an arbuscule (ar): the full arbuscule development and the integrity of the ER and nucleus (n) provide evidence of the root active symbiotic status and cell viability. Bars = 75 μm (A, C, E); 25 μm (B, D, F)**.**

Suppl. Figure 2. Transmission electron microscopy images of chitin labeling with gold-wheat-germ agglutin in the walls of *Trichoderma atroviride* and *Gigaspora gigantea*. A, *T. atroviride* (Ta, green) hyphae both in direct contact and inside *G. gigantea* (Gg, red). A strong chitin labelling is evident in the walls of both fungi. B, Magnification of *G. gigantea* wall reveals widespread gold

granules. Amorphous extrusions (arrowheads) are not labelled. C, Detail of *G. gigantea* wall grown in the absence of *T. atroviride* shows a comparable distribution of gold granules. D, Quantitative analysis of chitin labeling in *G. gigantea* walls in the presence (green) and absence (red) of *T. atroviride* colonization. Bars represent the average number of gold granules per square µm. Non parametric Kruskal-Wallis test for the analysis of variance (letters) indicated that the average values are not significantly different. Bars = 0,5 µm

Suppl. Figure 3. Fluorescence mean intensity in *T. atroviride ech42::gfp* strain (A) and *nag1::gfp* strain (B) grown in axenic conditions or dual culture with *G. gigantea*. The two strains express cytoplasmic GFP as a reporter of ECH42 (endochitinase) and NAG1 (N-acetylglucosaminidase) gene expression, respectively. Blue = axenic culture; red = dual culture 24 hpi (no hyphal contact), green = dual culture 96 hpi (extensive contact and mycoparasitism). Non parametric Kruskal-Wallis test for the analysis of variance revealed the absence of significant changes in the expression level of ECH42 during the whole time-course of the experiment. NAG1 expression level was weakly enhanced 24 hpi and then decreased to values lower then the axenic culture.

Suppl. Figure 4. Movie from a confocal microscope observation of *Gigaspora margarita* hyphae before exposure to UV irradiation. Viability of *G. margarita* hyphae is validated by the presence of strong cytoplasmic streams. Real-time duration = 1 min. Bars = 20 µm.

Suppl. Figure 5. Movie from a confocal microscope observation of *Gigaspora margarita* hyphae

after 1h30min exposure to UV irradiation. Non-viability of *G. margarita* hyphae is attested by the interruption of cytoplasmic streams. Real-time duration = 1 min. Bars = 20 µm.

Suppl. Figure 6. Movie from confocal microscope observation of the dual interaction between *Trichoderma atroviride* PKI1 (green) with the non-viable autofluorescent AM fungus *Gigaspora margarita* (orange) 72hpi of *T. atroviride. Trichoderma* hypha proceeds all along a *Gigaspora* hypha and branches in correspondence of the parasitized hyphal branches. Subsequent profuse branching lead to the occupation of most of the hyphal lumen The swelling of *Trichoderma* hyphal tip was evident as it reached the apex of the *Gigaspora* hypha. Eventually, *Trichoderma* exited the *G. margarita* apex by perforating its terminal wall. Frames were recorded every 10 minutes.

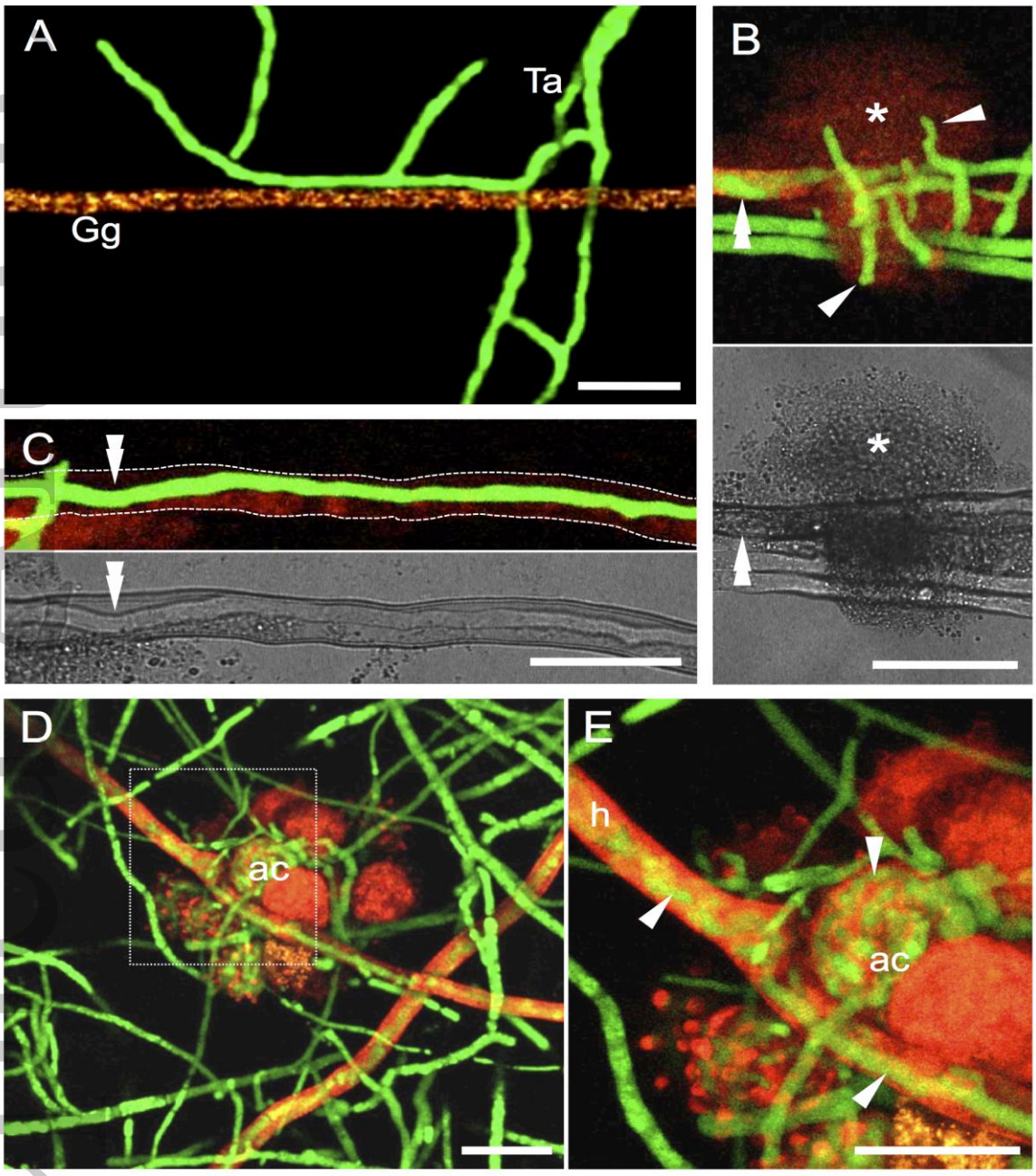

Figure 1. Interaction of *Trichoderma atroviride* strain P1 expressing the GFP protein (mutant PKI1) (green) with the autofluorescent AM fungus *Gigaspora gigantea* (red), observed in confocal laser microscopy 24 (A), 48 (B and C) and 72 (D and E) hours post inoculation. A, Contact between hyphae of *T. atroviride* (Ta), and *G. gigantea* (Gg). No specialized adhesion structures are recognizable associated with hyphal contact. B, Images of *G. gigantea* cytoplasmic rupture (asterisk) observed in fluorescence (top) and transmitted light (bottom) microscopy; presumably due to perforation of the hyphal cell wall by *T. atroviride* hyphae. The hypha of PKI1 is visible inside the AM fungal hypha (double arrowhead). Note the cluster of short branches (arrowheads) of PKI1 hyphae developed towards *G. gigantea* cytoplasmic outburst. C, *T. atroviride* (double arrowheads) growing inside a hypha of *G. gigantea* (dotted line), almost devoid of cytoplasm (as indicated by its low fluorescence), observed under fluorescence (top) and transmitted light (bottom). D, Extensive growth of *T. atroviride* mycelium around and inside *G. gigantea* hyphae and auxilliary cells (ac). E, Higher magnification of the area outlined in D, showing *T. atroviride* hyphae (arrowheads) growing inside the cytoplasm of *G. gigantea* hyphae (h) and auxiliary cells (ac). Bars = 25µm

727

728 EMI4_12221_F1

729

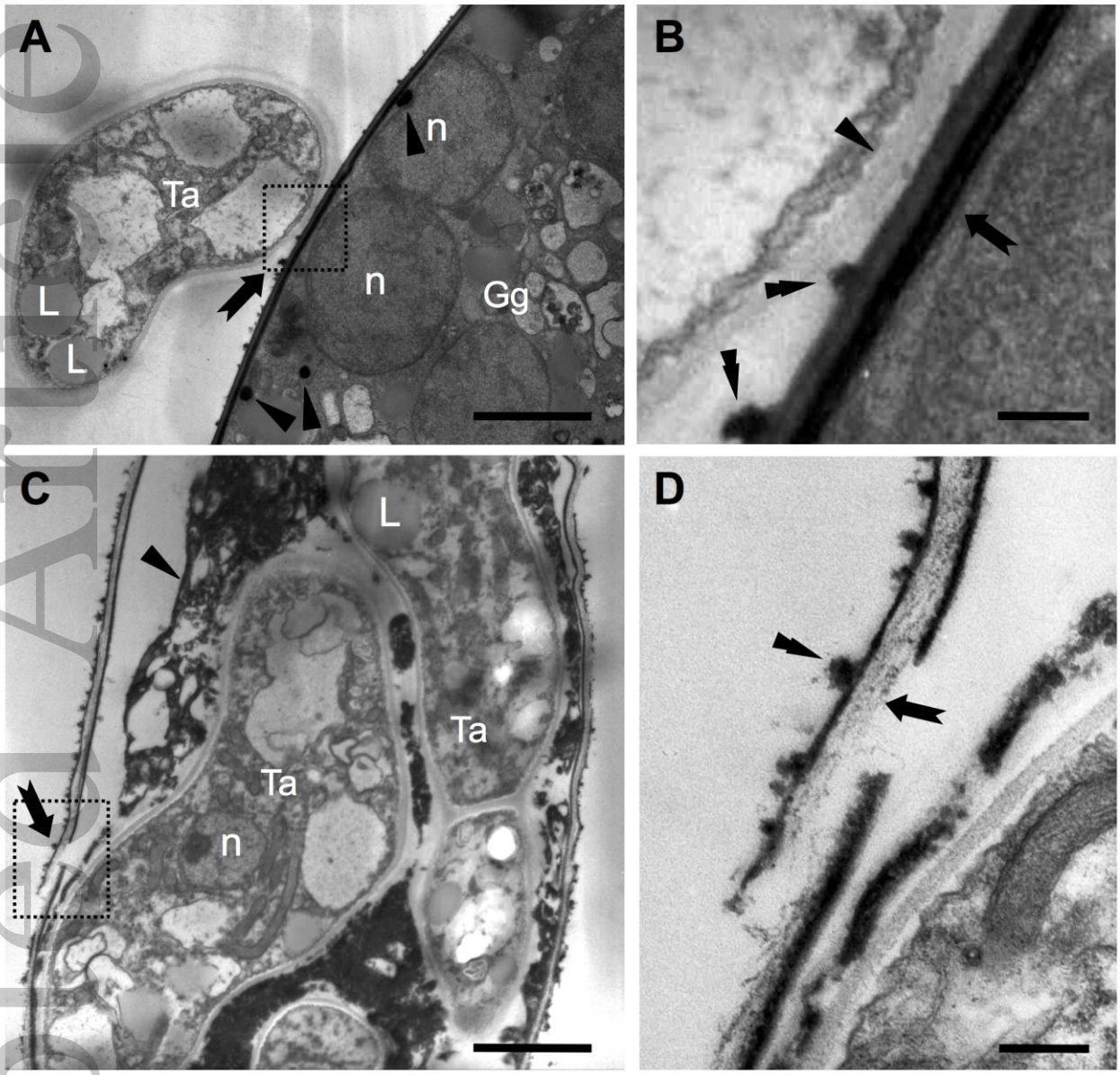

Figure 2. Transmission electron microscopy images of the dual interaction between *Trichoderma atroviride* and *Gigaspora gigantea.* A, Direct contact between the two fungal walls (arrow and boxed area). Both *T. atroviride* (Ta) and *G. gigantea* (Gg) hyphae have healthy cytoplasms with easily recognizable organelles: intact nuclei (n), lipid globules (L) and electron dense granules (arrowheads). B, Higher magnification of the area boxed in A, showing the contact between the electron-transparent wall of *T. atroviride* (arrowhead) and the electron-dense wall of *G. gigantea* (arrow) displaying two distinct dark layers. Amorphous masses (double arrowheads) emerge from the outer layer of the AM fungus. C, *G. gigantea* hypha colonized by *T. atroviride*. The AM hyphal wall is partially degraded (arrow and boxed area); cytoplasm is collapsed into a degenerated mass (arrowhead), and the organelles are no longer distinguishable; by contrast, *T. atroviride* hyphae (Ta) appear healthy and active, displaying nuclei (n) and lipid globules (L). D, Higher magnification of the area boxed in C, showing a site of wall damage in *G. gigantea*: the inner electron-dense layer is replaced by a loose fibrillar matrix (arrow). By contrast, the wall external layer and amorphous masses (double arrowhead) are not degraded. Bars = 2 µm (A and C); 1 µm (B and D).

EMI4_12221_F2

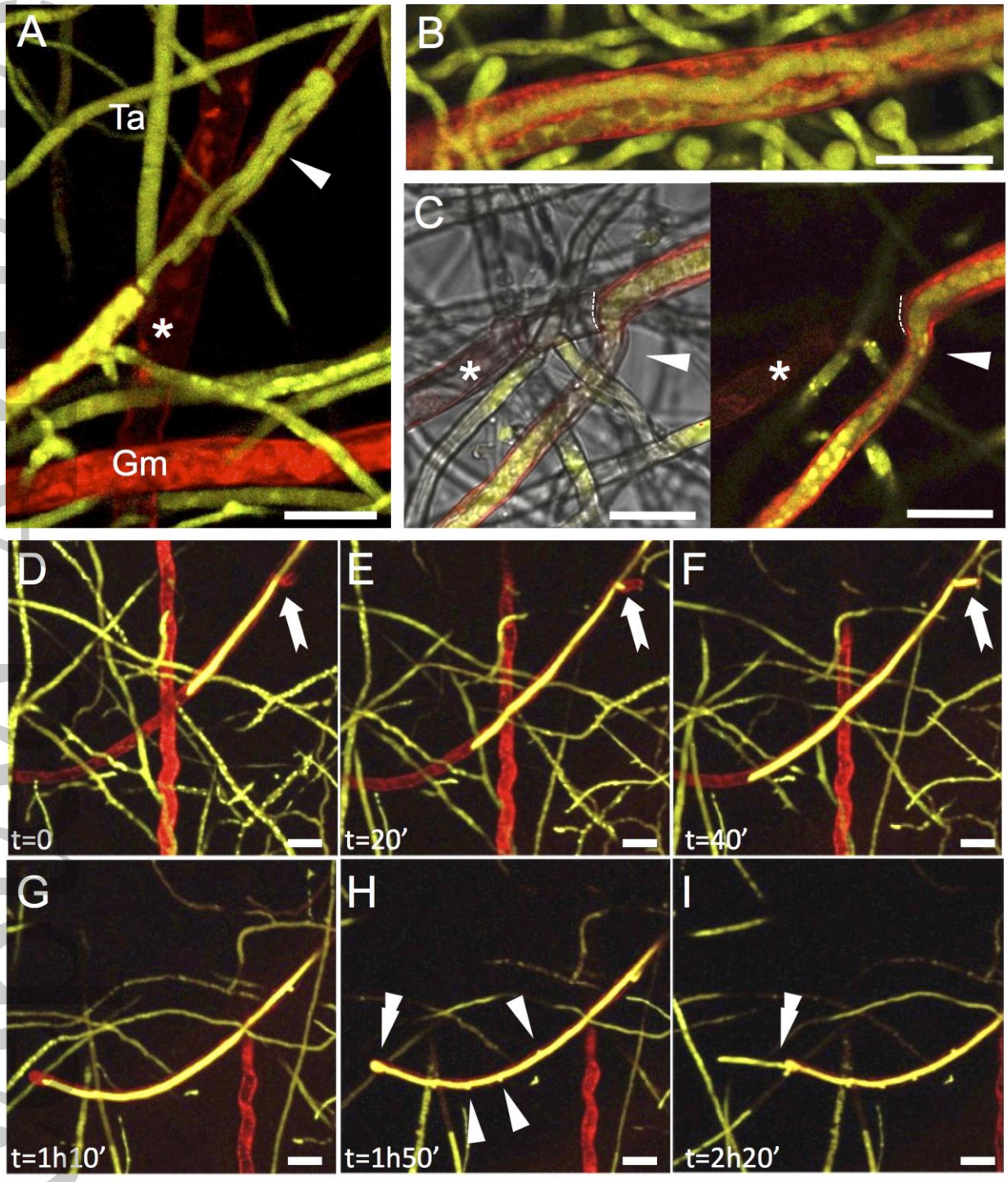

Figure 3. Interaction of *Trichoderma atroviride* PKI (green) with non-viable (UV-treated) hyphae of *Gigaspora margarita* (red), observed in confocal microscopy after inoculation of *T. atroviride*. A, B 48 hpi, *T. atroviride* (green) extensively colonized *G. margarita* (red) with intra-hyphal coils (arrowhead). C Preferential growth of *T. atroviride* inside cytoplasm-filled hyphae of *G. margarita* (arrowhead) observed in fluorescence (right) and transmitted light (left) 72 hpi: a hyphal branch devoid of cytoplasm (asterisk), delimited by a septum (dotted line), is not colonized by *T. atroviride.* D-I, Time-lapse series (total duration = 2h20') showing *T. atroviride* growing inside *G. margarita* hyphae. D-F, Branching of *T.atroviride* within a *G. margarita* hyphal branch. H-I. Swelling and outbreak of *T.atroviride* hyphal tip at the apex of the *G. margarita* hypha (double arrowhead). Note the profuse branching of *T. atroviride* (H, arrowheads) inside the parasitized hyphae. Bars = 20µm

733

734 EMI4_12221_F3

735

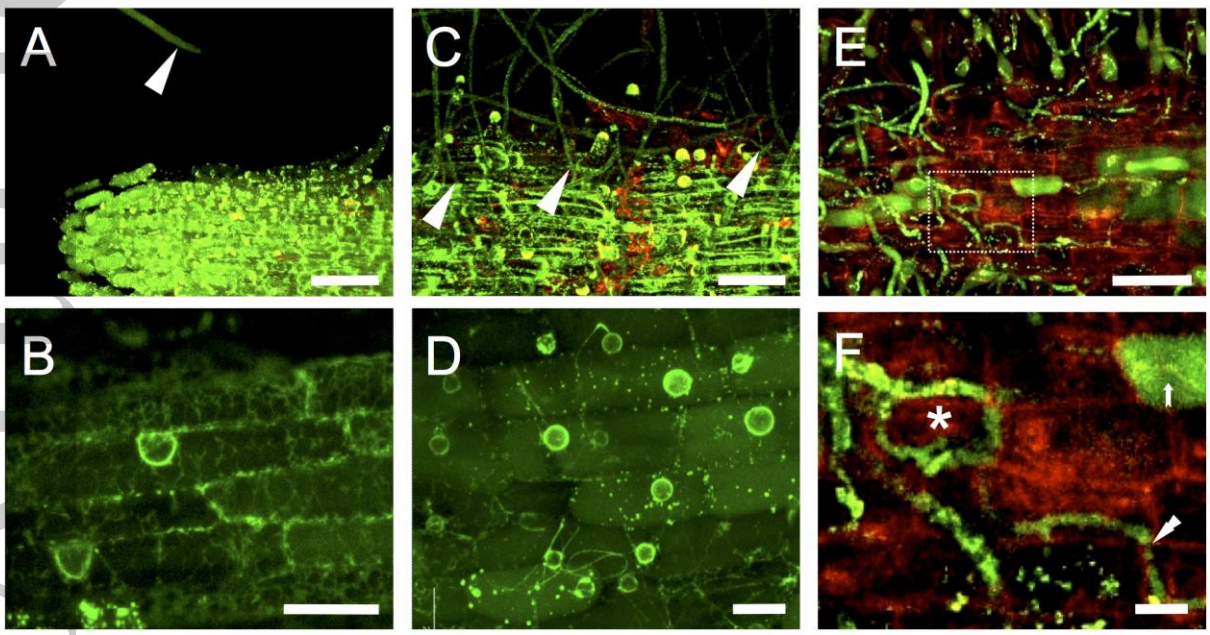

Figure 4. Dual interaction of *Trichoderma atroviride* PKI1 constitutively expressing cytoplasmic GFP (green) with root organ cultures of *Medicago truncatula* expressing GFP-HDEL as a marker of the endoplasmic reticulum. All images are obtained in confocal microscopy. A, B, 48 hpi of *T. atroviride,* a hypha (arrowhead) is approaching *M. truncatula* root. The intense fluorescence and integrity of the endoplasmic reticulum lace-like network (B) is a clear indicator of plant cell viability. C, D, 72 hpi, hyphae of the rapidly expanding *T. atroviride* mycelium overlap and coil around the root. Several contacts between hyphae and the root epidermis are visible (arrowheads) but no specialized adhesion structure is recognizable. The partial disorganization of the endoplasmic reticulum is evident in D, in the form of isolated patches and spots of GFP fluorescence. E, F, Six days after *T. atroviride* inoculum, most of the contacted epidermal cells are dead, as indicated by the partial to total disruption of the endoplasmic reticulum, and the disappearance or diffusion (arrow) of GFP fluorescence. Some of the hyphae are visible in F, coiling inside an epidermal cell (asterisk) and growing from cell to cell (double arrowhead). The weak red fluorescence of the plant cell walls becomes apparent in these images due to the absence of the bright GFP signal. Bars = 75 µm (A, C, E); 12µm (B, D, F).

736

737 EMI4_12221_F4

738

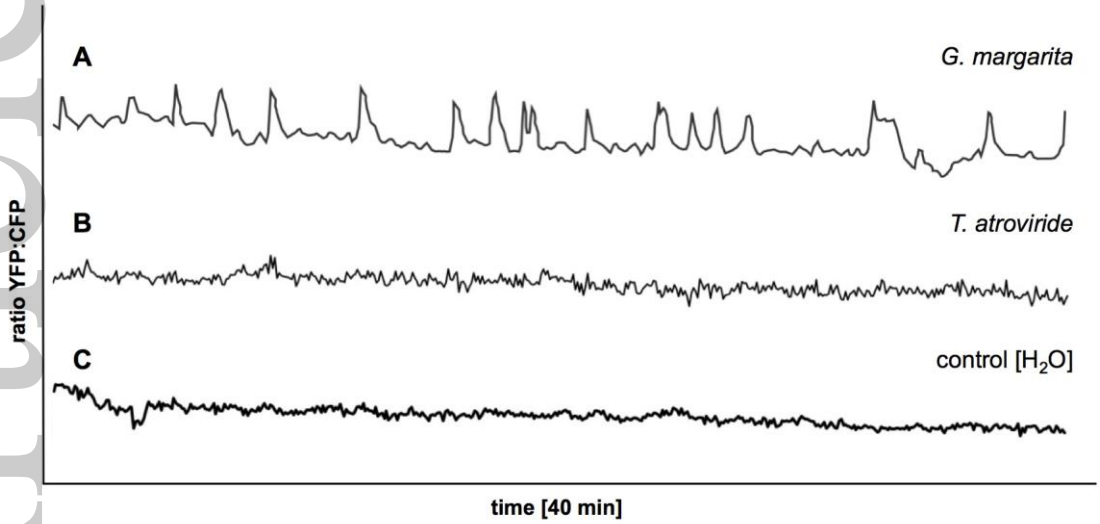

Figure 5. Fluorescence resonance energy transfer (FRET) plots representing nuclear Ca^{2+} levels in epidermal cells of *Medicago truncatula* root organ cultures treated with culture filtrates of *Gigaspora margarita* (A), *Trichoderma atroviride* PKI1 (B), or sterile water as control (C). A, Treatment with 10 times concentrated exudate from germinated *Gigaspora margarita* spores elicits intense spiking over the 40-min acquisition period. B, By contrast, no oscillation is visible in the plots from roots exposed to 10 times concentrated *T. atroviride* culture filtrates. C, No Ca^{2+} signals are elicited in control treatments with sterile water.

739

740 EMI4_12221_F5

741

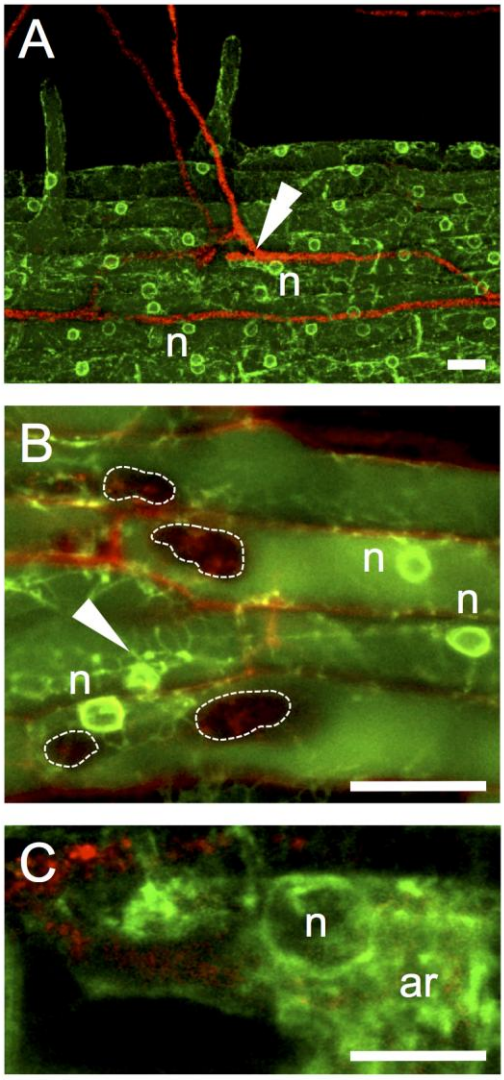

Figure 6. AM colonization of *Medicago truncatula* GFP-HDEL root organ cultures by *Gigaspora gigantea* before the inoculation of *Trichoderma atroviride* PKI1, observed in confocal microscopy. A, *Gigaspora gigantea* hyphopodium (double arrowhead) adhering to the root epidermis. Root cells display a healthy endoplasmic reticulum (note that GFP labelling extends to the nuclear envelope (n). B, Single optical section from the root cortical tissue. Cells colonized by *G. gigantea* hyphae (outlined by dotted lines) have an intact nucleus (n) and endoplasmic reticulum network (arrowhead). C, Optical section from an inner cortical cell hosting an arbuscule (ar), indicative of the active status of the symbiosis. The large nucleus (n) and arbuscule branches are surrounded by the intense GFP signal accumulated in the lumen of the nuclear envelope and ER respectively. Bars = 25μm.

742

743 EMI4_12221_F6

744

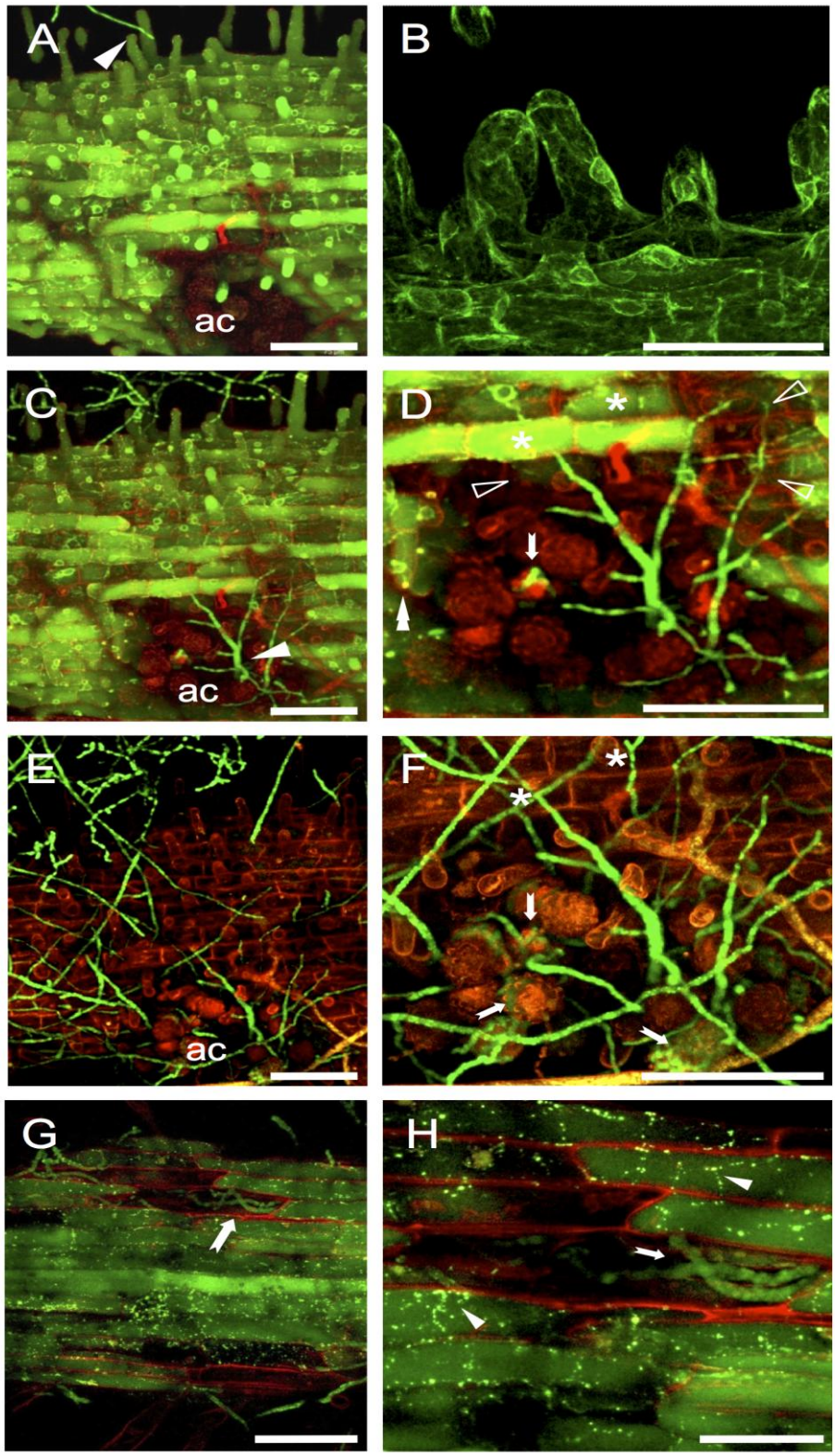

EMI4_12221_F7